*Revista Mexicana de Astronomía y Astrofísica*, **39**, 41–53 (2003)

# CCD PHOTOMETRY OF THE OPEN CLUSTERS NGC 2658, NGC 2849, AND NGC 3247

J. A. Ahumada[1]

Observatorio Astronómico, Universidad Nacional de Córdoba, Argentina

*Received 2002 April 23; accepted 2003 February 18*



RESUMEN

Presentamos fotometría CCD de los cúmulos abiertos galácticos NGC 2658, NGC 2849 y NGC 3247. Por medio de la comparación entre las secuencias observadas y las isócronas teóricas de Padua, derivamos los siguientes parámetros. Para NGC 2658 obtenemos: $E(B-V) = 0.35^{+0,05}_{-0,10}$, $\log(\text{edad}) = 8.50^{+0,25}_{-0,05}$ y $(m-M)_0 = 13.32^{+0,36}_{-0,52}$. En el caso de NGC 2849 el enrojecimiento cubre el rango de 0,46 a 0,57 con una incerteza de ±0.12 mag, $(m-M)_0 = 14.02^{+0,38}_{-0,40}$, en tanto que $\log(\text{edad}) = 8.8^{+0,1}_{-0,05}$. Finalmente, para NGC 3247 derivamos: $E(B-V) = 0.39 \pm 0.07$, $\log(\text{edad}) = 7.6^{+0,4}_{-0,3}$, y $(m-M)_0 = 11.89^{+0,51}_{-0,45}$. En este estudio las isócronas han sido renormalizadas a los valores solares $(B-V)_\odot = 0.65$ y $M_V = 4.84$; se proponen además los valores $(V-R)_\odot = 0.37$ y $(V-I)_\odot = 0.70$ como puntos de referencia para también renormalizar dichos colores.

ABSTRACT

We present CCD photometry of the galactic open clusters NGC 2658, NGC 2849, and NGC 3247. By means of the comparison between the observed cluster sequences and the Padova theoretical isochrones, we derive the following parameters: for NGC 2658, $E(B-V) = 0.35^{+0.05}_{-0.10}$, $\log(\text{age}) = 8.50^{+0.25}_{-0.05}$, and $(m-M)_0 = 13.32^{+0.36}_{-0.52}$; for NGC 2849, the reddening is in the range 0.46 to 0.57 with an uncertainty of ±0.12 mag, $(m-M)_0 = 14.02^{+0.38}_{-0.40}$, and $\log(\text{age}) = 8.8^{+0.1}_{-0.05}$; finally, for NGC 3247 we obtain $E(B-V) = 0.39 \pm 0.07$, $\log(\text{age}) = 7.60^{+0.4}_{-0.3}$, and $(m-M)_0 = 11.89^{+0.51}_{-0.45}$. In this study the isochrones have been renormalized to the solar values $(B-V)_\odot = 0.65$ and $M_V = 4.84$; the values $(V-R)_\odot = 0.37$ and $(V-I)_\odot = 0.70$ are proposed as zero points in order to renormalize those colors as well.

*Key Words:* **OPEN CLUSTERS AND ASSOCIATIONS: GENERAL — OPEN CLUSTERS AND ASSOCIATIONS: INDIVIDUAL (NGC 2658, NGC 2849, NGC 3247)**

## 1. INTRODUCTION

The southern, galactic open clusters NGC 2658, NGC 2849, and NGC 3247 have different records of observations. NGC 2658 (C0841 − 324) is located at $l = 254.^\circ56$, $b = -6.^\circ07$; it is relatively bright, extended and rich. Ramsay & Pollaco (1992) find, based on a CCD *UBV* photometry, an age of $\sim 2 \times 10^8$ yr ($\log \text{age} = 8.3$), $E(B-V) = 0.40$, and a distance of 3.8 kpc.

NGC 3247 (C1024−076) apparently does not have a standard Johnson photometry. Grubissich (1977), from photographic *RGU* observations, gets an age of $\sim 5 \times 10^7$ yr ($\log \text{age} = 7.7$), $E(G-R) =$

[1]Visiting Astronomer, University of Toronto Southern Observatory, and Complejo Astronómico El Leoncito, operated under agreement between the Consejo Nacional de Investigaciones Científicas y Técnicas de la República Argentina, and the National Universities of La Plata, Córdoba, and San Juan.

0.35, and a distance of 1420 pc. This cluster is at $l = 284.^{\circ}57$, $b = -0.^{\circ}34$, is somewhat brighter than NGC 2658, but poorer in stars.

Finally, there seems to be no photometry of NGC 2849 (C0917−403). It is a small and faint cluster at $l = 265.^{\circ}27$, $b = +6.^{\circ}36$. Its apparent diameter is $3'$ and the Trumpler class is I1m (Lyngå 1987).

In this paper we present new, multicolor CCD photometry of the three clusters, and derive their fundamental parameters through the comparison with the theoretical models published by the Padova group (Bertelli et al. 1994; Girardi et al. 2000).

## 2. OBSERVATIONS

The observations were carried out at two places: (i) The Complejo Astronómico El Leoncito (CASLEO), San Juan, Argentina. The instrument is the 2.15 m Jorge Sahade Telescope; the detector is a TEK-1024 CCD, and the filters are standard *BVRI* Johnson-Cousins. The images cover a circle of ∼ 9 arcmin of diameter; the scale is 0.813 arcsec/pixel. (ii) The University of Toronto Southern Observatory, at Las Campanas, Chile. In this case the instrument is the 0.60 m Helen Sawyer Hogg Telescope; the detector is a CCD PM 512×512, the scale on the chip is 0.45 arcsec/pixel, and the observed field is a square of about $4' \times 4'$; the filters are also standard *BVRI*.

Our procedure is as follows. Three identical exposures per filter are made and combined; if necessary, there are short exposures in some filters to measure bright stars. We observe the same cluster field on two different nights in order to cross-check the internal consistency of our photometry and combine the data when possible. Our results are finally compared with published photometry, if it exists. Some details of the observations are given in Table 1; the times listed are those of the middle of the second exposure.

**NGC 2658.** Observations of this cluster were carried out from CASLEO on the nights of 8–9 January 1997 and 18–19 April 2001, in the *BVRI* filters. The average full-width half maxima (FWHM) of the stellar images are 2.4 and 3.2 arcsec, and the ranges of airmasses are 1.01–1.05 and 1.13–1.29, respectively. A comparison field at $\sim 20'$ toward the south of the cluster was also observed on the first night.

**NGC 2849.** Data in the *BVRI* filters were obtained at Las Campanas on the night 10–11 April 1996, and at CASLEO on 19–20 April 2001. The mean FWHM are 2.0 and 3.7 arcsec, respectively. The airmasses are ∼ 1.02 for Las Campanas and 1.06–1.13 for CASLEO.

**NGC 3247.** This cluster was observed at CASLEO on the nights 16–17 January 1996 (*BV*) and 1–2 April 1998 (*BVI*). The FWHM of the stellar images are, respectively, 3.6 and 2.6 arcsec. The airmasses are 1.11 for the first night and 1.29–1.36 for the second. A comparison field was observed on the first night at $\sim 10'$ toward the north.

**Standard Stars.** To do absolute photometry, Graham (1982) standard stars were observed each night. The brightest ($V \sim 8$–11) could be observed at Las Campanas, while stars fainter than $V \sim 12$ were suitable for the larger telescope at CASLEO. The range of $(B-V)$ goes from ∼ 0.05 to ∼ 1.25. Typically, about twelve standard stars were observed per night at Las Campanas, and more than twenty at CASLEO. In all cases the standards were observed along the whole night. The ranges of airmasses covered by these observations are: 16–17 January 1996, 1.03–1.66; 10–11 April 1996, 1.04–1.22; 8–9 January 1997, 1.03–1.16; 1–2 April 1998, 1.03–1.33; 18–19 April 2001, 1.03–1.24; 19–20 April 2001, 1.07–1.32.

## 3. PHOTOMETRY

The pre-processing of the raw data, as well as the photometry itself, were carried out inside IRAF.[2] The photometric package utilized is thus DAOPHOT (Stetson 1987, 1990), and the procedure followed is standard. Aperture photometry is performed to obtain instrumental magnitudes of standard stars. In program frames, profile-fitting photometry is instead performed, through the construction of the frame point-spread function (PSF). The zero point of the instrumental magnitudes for each image is determined with small-aperture photometry and growth curves.

To bring the instrumental magnitudes to the standard system, the proper equations for all nights and observatories are of the form

$$M = m + c_0 + c_1 \times X + c_2 \times C, \qquad (1)$$

where $M$ and $m$ are the standard and instrumental magnitudes, respectively, $X$ is the airmass, $C$ is an appropriate standard color index, and $c_i$ are the zero point, first-order extinction, and color term coefficients. A second-order extinction term does not seem to improve the fit. The $C$ indexes are: $(B-V)$ for $B$ and $V$, $(V-R)$ for $R$, and $(R-I)$ for $I$. In each observing run, the nightly $c_0$ and $c_2$

[2]IRAF is distributed by the National Optical Astronomy Observatories which are operated by the Association of Universities for Research in Astronomy, Inc., under cooperative agreement with the National Science Foundation.

TABLE 1

OBSERVATIONS

| Cluster | Date | Filter | Exposure (s) | UT (h m) |
|---|---|---|---|---|
| NGC 2658 | 9 Jan 1997 | $R$ | 40 | 6 50 |
| | | $I$ | 40 | 7 05 |
| | | $B$ | 100 | 7 16 |
| | | $V$ | 60 | 7 27 |
| | 19 Apr 2001 | $V$ | 60 | 1 43 |
| | | $B$ | 100 | 1 57 |
| | | $I$ | 40 | 2 28 |
| | | $R$ | 50 | 2 34 |
| NGC 2849 | 11 Apr 1996 | $B$ | 200 | 1 00 |
| | | $V$ | 100 | 1 10 |
| | | $R$ | 60 | 1 16 |
| | | $I$ | 45 | 1 25 |
| | 20 Apr 2001 | $V$ | 60 | 1 28 |
| | | $B$ | 100 | 1 37 |
| | | $I$ | 30 | 2 07 |
| | | $R$ | 40 | 2 16 |
| NGC 3247 | 17 Jan 1996 | $B$ | 100 | 7 13 |
| | | $V$ | 60 | 7 20 |
| | 2 Apr 1998 | $B$ | 60 | 5 20 |
| | | $V$ | 50 | 5 27 |
| | | $I$ | 30 | 5 42 |

coefficients can be averaged, since in principle they should remain approximately constant. With these mean values, the extinction coefficients $c_1$ can be recalculated. The $c_1$'s are in principle expected to vary on a nightly basis, as they depend on the extinction, but in fact they proved to be quite constant during the observing runs, and thus they were averaged as well. The mean coefficients are listed in Table 2, while in Table 3 are the ranges of rms errors of the individual transformations for each observing run. For the nights in consideration, the rms errors are: 16–17 January 1996, 0.023 ($B$), 0.016 ($V$); 10–11 April 1996, 0.012 ($B$), 0.008 ($V$), 0.013 ($R$), 0.017 ($I$); 8–9 January 1997, 0.008 ($B$), 0.019 ($V$), 0.015 ($R$), 0.014 ($I$); 1–2 April 1998, 0.024 ($B$), 0.025 ($V$), 0.017 ($I$); 18–19 April 2001, 0.011 ($B$), 0.010 ($V$), 0.017 ($R$), 0.019 ($I$); 19–20 April 2001, 0.015 ($B$), 0.014 ($V$), 0.018 ($R$), 0.015 ($I$).

The comparison between the photometries of the same cluster obtained on different nights results in no apparent trend along $V$ in any of the three cases.

TABLE 2

MEAN COEFFICIENTS FOR THE TRANSFORMATION EQUATIONS

| | $c_0$ | $\sigma$ | $c_1$ | $\sigma$ | $c_2$ | $\sigma$ |
|---|---|---|---|---|---|---|
| Las Campanas, April 1996 (7 nights) | | | | | | |
| $B$ | +2.13 | 0.03 | −0.19 | 0.03 | +0.122 | 0.003 |
| $V$ | +1.66 | 0.02 | −0.16 | 0.02 | +0.038 | 0.003 |
| $R$ | +1.15 | 0.03 | −0.13 | 0.02 | −0.036 | 0.006 |
| $I$ | +1.09 | 0.03 | −0.14 | 0.02 | +0.090 | 0.007 |
| CASLEO, January 1996 (3 nights) | | | | | | |
| $B$ | +1.33 | 0.04 | −0.26 | 0.03 | +0.132 | 0.011 |
| $V$ | +2.68 | 0.03 | −0.24 | 0.04 | +0.014 | 0.018 |
| CASLEO, January 1997 (5 nights) | | | | | | |
| $B$ | +1.26 | 0.06 | −0.19 | 0.06 | +0.091 | 0.014 |
| $V$ | +2.64 | 0.08 | −0.19 | 0.08 | −0.066 | 0.010 |
| $R$ | +2.73 | 0.07 | −0.10 | 0.06 | +0.033 | 0.017 |
| $I$ | +1.78 | 0.06 | −0.10 | 0.06 | +0.026 | 0.022 |
| CASLEO, April 1998 (3 nights) | | | | | | |
| $B$ | +2.41 | 0.04 | −0.22 | 0.03 | +0.019 | 0.010 |
| $V$ | +3.41 | 0.05 | −0.21 | 0.04 | +0.017 | 0.011 |
| $R$ | +3.14 | 0.05 | −0.06 | 0.04 | +0.014 | 0.021 |
| $I$ | +2.53 | 0.04 | −0.17 | 0.04 | −0.054 | 0.020 |
| CASLEO, April 2001 (4 nights) | | | | | | |
| $B$ | +2.25 | 0.03 | −0.24 | 0.03 | +0.019 | 0.006 |
| $V$ | +3.20 | 0.03 | −0.18 | 0.03 | +0.013 | 0.006 |
| $R$ | +3.03 | 0.04 | −0.13 | 0.03 | +0.026 | 0.014 |
| $I$ | +2.21 | 0.04 | −0.05 | 0.03 | −0.012 | 0.019 |

The mean differences along the whole range of $V$, always in the sense of first night minus the second, are:

**NGC 2658** $\Delta V = +0.001 \pm 0.013$, $\Delta(B-V) = -0.036 \pm 0.012$, $\Delta(V-R) = -0.028 \pm 0.011$, $\Delta(V-I) = -0.021 \pm 0.016$ (732 stars);

**NGC 2849** $\Delta V = -0.033 \pm 0.015$, $\Delta(B-V) = -0.009 \pm 0.017$, $\Delta(V-R) = -0.032 \pm 0.016$, $\Delta(V-I) = -0.009 \pm 0.023$ (131 stars);

**NGC 3247** $\Delta V = +0.026 \pm 0.013$, $\Delta(B-V) = -0.040 \pm 0.014$ (402 stars).

Each pair of data sets is then merged into a single list. For this purpose, we make use of a program that averages the individual colors and magnitudes of the stars that are identified in both lists. The data are weighed by the photometric errors, since in general the nights are of different quality (as illustrated e.g.,

TABLE 3

RANGE OF RMS ERRORS OF THE TRANSFORMATIONS (UNITS OF $10^{-3}$)

| Obs. run | $B$ | $V$ | $R$ | $I$ |
|---|---|---|---|---|
| Jan 1996 | 13–23 | 16–17 | | |
| Apr 1996 | 6–19 | 7–14 | 7–13 | 9–17 |
| Jan 1997 | 7–33 | 8–23 | 12–27 | 8–22 |
| Apr 1998 | 19–25 | 20–25 | 19–26 | 16–20 |
| Apr 2001 | 14–26 | 13–28 | 13–21 | 19–23 |

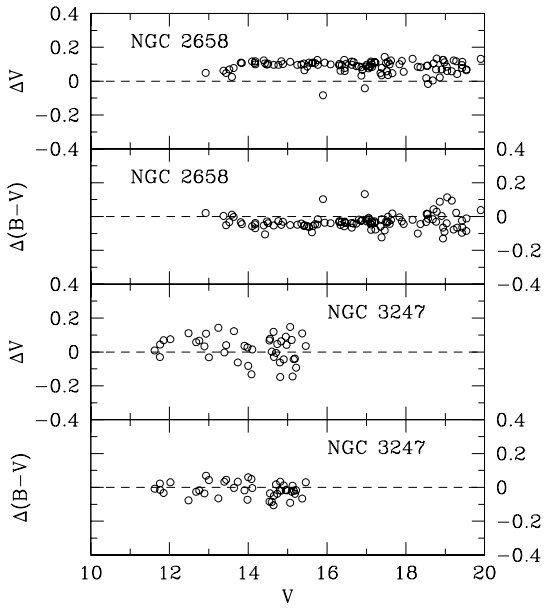


Fig. 1. Differences between our measurements and published photometry. The references are: for NGC 2658, Ramsay & Pollaco (1992); for NGC 3247, Grubissich (1977). Abscissae give our $V$ magnitude.

by the FWHMs of the stellar images), and the corresponding errors are also different. The stars are matched by their coordinates, $V$, and $(B-V)$. A star that appears in one list may not find a match in the other, due essentially to two reasons: the areas of sky observed on both occasions are not exactly the same, or the measurements differ. To allow for the last factor, we fixed intervals of tolerance based on the typical errors in the photometry and the transformations. If a star has a match according to its coordinates, but the difference in $V$ and/or $(B-V)$ exceeds the tolerance, only the star with the smallest photometric error is kept in the final list.

Our averaged data can now be compared with the published photometry, which is taken directly from the open cluster database *BDA* (Mermilliod 1995). The differences, in the sense of our photometry minus published photometry, are illustrated in Figure 1. Again, no trends with $V$ are observed, and the mean differences are the following.

**NGC 2658** Comparison with 105 stars also observed by Ramsay & Pollaco (1992), and over the range $13 < V < 20$, gives: $\Delta V = +0.088 \pm 0.012$, $\Delta(B-V) = -0.035 \pm 0.011$; for the bright star 1 (number 118 in BDA), the differences are: $\Delta V = 0.049$ mag, and $\Delta(B-V) = 0.021$ mag.

**NGC 3247** In order to compare with the *RGU* photographic photometry of Grubissich (1977), we transformed his colors to Johnson $BV$ with the equations given in Golay (1974), using $E(G-R) = 0.35$. Along the range $11 < V < 16$, and for 42 stars, the mean differences are: $\Delta V = +0.042 \pm 0.024$, and $\Delta(B-V) = -0.010 \pm 0.015$, quite good given the uncertainties in the transformation of the old data.

Figure 2 shows the $V$ versus $(B-V)$ and $V$ versus $(V-I)$ color-magnitude diagrams of the three clusters, as well as the $V$ versus $(B-V)$ diagrams of the comparison fields. Tables 4 to 6[3] list the final photometric data. In them, the stars are arranged by $V$; their coordinates $(x, y)$ are also given, relative to a center set by visual inspection. The identification charts are in Figure 3.

## 4. ANALYSIS

### 4.1. *Renormalization of Isochrones*

Our analysis of the color-magnitude diagrams is essentially based on the well-known method of isochrone-fitting. In this study we make use of the isochrones computed by Girardi et al. (2000). The models cover a wide range of metallicities, and the evolutionary tracks include the core-He burning stage. The solar model has been calibrated adopting a metal content $Z_\odot = 0.019$, an overshooting parameter $\Lambda_e = 0.25$, and a mixing-length parameter $\alpha = 1.68$. However, this set does not include isochrones younger than $\log t = 7.80$. L. Girardi (`http://pleiadi.pd.astro.it`) suggests that, in such a case, the isochrones by Bertelli et al. (1994) can be used, at least when the compositions are the same.

VandenBerg & Poll (1989), when fixing the position of a semi-empirical ZAMS, adopt for the present

[3]Available at CDS: `http://vizier.u-strasbg.fr/cgi-bin/VizieR-2?-source=J/other/RMxAA/39.39` or `ftp://cdsarc.u-strasbg.fr/pub/J/other/RMxAA/39.39`.

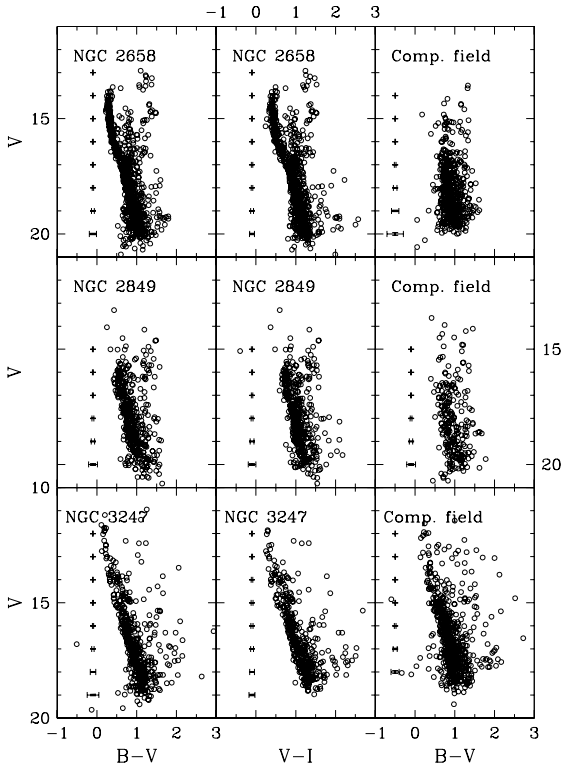


Fig. 2. Color-magnitude diagrams of NGC 2658, NGC 2849, and NGC 3247, and of their comparison fields. All observed stars in the fields centred on NGC 2658 and NGC 3247 are plotted. Stars up to 3′ from the center of NGC 2849 are plotted, while its comparison field diagram shows the stars beyond 3′. The error bars in these and other color-magnitude diagrams represent averages of the individual photometric errors of the measurements, in the correspondings intervals of magnitude and color.

sun the values $M_V = 4.84$ and $(B-V)_\odot = 0.64$, provided that $Y = 0.27$ and [Fe/H]=0.0. This zero point has been subsequently used (cf. e.g., Twarog & Anthony-Twarog 1989, 1993; Twarog, Ashman, & Anthony-Twarog 1997), albeit slightly modified (they assume $(B-V)_\odot = 0.65$), to standardize different sets of isochrones. This is justified by the fact that, despite the care taken by the authors in calibrating the solar model, differences appear in the transformation of the evolutionary tracks onto the observational plane (for instance, see the discussion at the beginning of Appendix A of Twarog et al. 1997). If the isochrones are renormalized, meaningful comparisons among the results derived from their use can be made, regardless of how exact are the solar colors chosen as zero points. As Twarog et al. (1997) say, to shift a whole set of isochrones of all

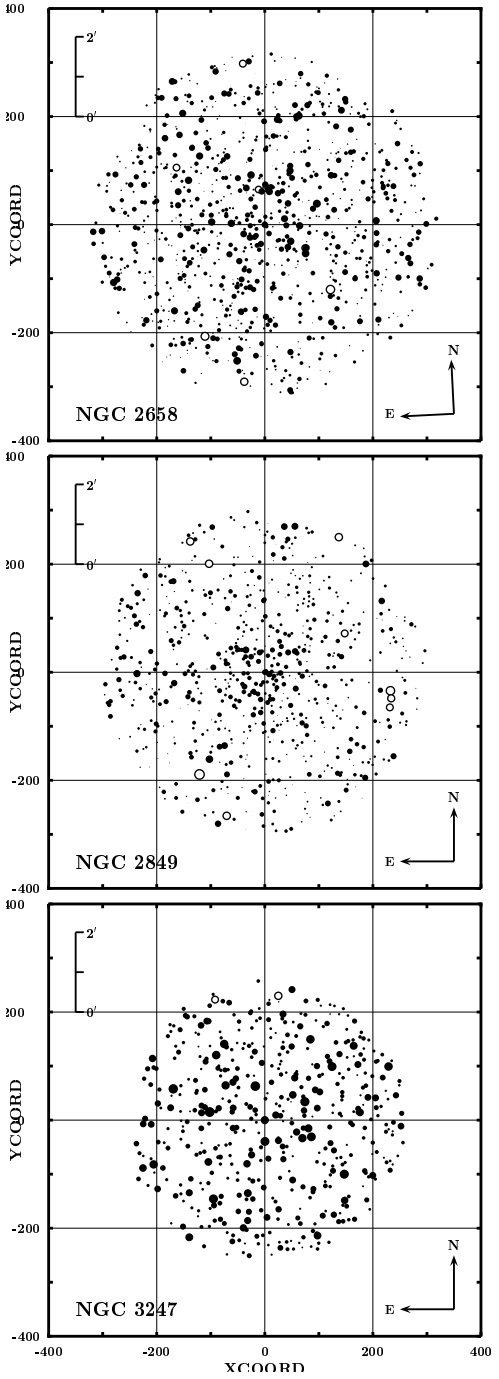


Fig. 3. Identification charts of NGC 2658, NGC 2849, and NGC 3247. The brightest stars (open circles) are added for the sake of completeness. The coordinates of the centers are: NGC 2658, $\alpha_{2000.0} = 08^{\rm h}43\overset{\rm m}{.}4$, $\delta_{2000.0} = -32^\circ\,39\overset{\prime}{.}9$; NGC 2849, $\alpha_{2000.0} = 09^{\rm h}19\overset{\rm m}{.}4$, $\delta_{2000.0} = -40^\circ 31\overset{\prime}{.}2$; NGC 3247, $\alpha_{2000.0} = 10{\rm h}26\overset{\rm m}{.}9$, $\delta_{2000.0} = -57^\circ 55\overset{\prime}{.}7$.

ages and metallicities in such a way that a solar mass star at 4.6 Gyr, with $Y = 0.27$ and [Fe/H]=0.0, has $M_V = 4.84$ and $(B-V) = 0.65$, is the simplest, although not technically the most correct, means of standardizing the entire set.

We wish to tie our study to that performed by the authors cited above, because we think it is worthwhile trying to obtain cluster parameters in a (at least) differentially consistent way; besides, we can take advantage of the fact that the reference point has already been established.

Consequently, we have to determine the offsets of the Padova isochrones. First, we determine the theoretical solar colors by means of a linear interpolation between the appropriate isochrones. For Girardi et al. (2000), the interpolation is performed between the isochrones of solar metallicity for $\log t = 9.65$ ($t = 4.5$ Gyr) and $\log t = 9.70$ ($t = 5$ Gyr), and thus we derive for the present sun ($t = 4.6$ Gyr, mass = 1) the magnitude $M_V = 4.85$, and the colors $(B-V) = 0.673$, $(V–R) = 0.378$, and $(V–I) = 0.726$. In the case of Bertelli et al. (1994), from the isochrones of solar metallicity and $\log t = 9.60$ ($t = 4$ Gyr) and 9.70, we derive $M_V = 4.87$, $(B-V) = 0.68$, $(V-R) = 0.38$, and $(V-I) = 0.73$.

Secondly, since in our analysis we use the $(V-R)$ and $(V–I)$ indexes besides $(B–V)$, we must fix the reference colors $(V–R)_\odot$ and $(V–I)_\odot$. We are not, however, aware of suitable colors that have been chosen for a purpose like this, and consequently we propose the following procedure to derive them. Alonso, Arribas, & Martínez-Roger (1996) have calibrated the effective temperatures versus metallicity and several color indexes for low main sequence stars ranging in spectral type from F0 to K5. They obtain a number of equations that give, assuming $T_{\rm eff}$ and [Fe/H], the required color index. For our purposes, we use, in first place, their relationship $T_{\rm eff}$ : [Fe/H] : $(B–V)$ to derive a $T_{\rm eff}$ appropriate for $(B–V)_\odot = 0.65$. It turns out to be $T_{\rm eff} = 5660.3297$ K, or $\theta_{\rm eff} = 5040/T_{\rm eff} = 0.8904075$. Next, we enter this effective temperature in the $T_{\rm eff}$ : [Fe/H] : $(V–R)$ and $T_{\rm eff}$ : [Fe/H] : $(R–I)$ relationships to derive the corresponding $(V-R)_\odot$ and $(R-I)_\odot$ indexes, consistent with the assumed $(B-V)_\odot$. Finally, as the indexes obtained are in the Johnson system, they are transformed into the Cousins system as indicated by Bessell (1983). The resultant indexes are: $(V-R)_\odot = 0.373$ and $(V-I)_\odot = (V-R)_\odot + (R-I)_\odot = 0.698$. We propose that they be approximated to 0.37 and 0.70 mag, respectively, and that they be adopted as zero points. All the reference solar colors are shown in Table 7.

Before obtaining the offsets, a small correction to $M_V$ must be introduced due to the fact that the solar isochrones by Girardi et al. (2000) and Bertelli et al. (1994) are respectively computed with $Y = 0.273$ and $Y = 0.28$, and the zero point is defined for $Y = 0.27$. The corrections can be calculated with eq. (3) of VandenBerg & Poll (1989), and amount to +0.008 and +0.026 mag, respectively. It is worth noting that the $Z$ values of both solar sets of isochrones are assumed to be correct for $[Fe/H] = 0.0$ (see Twarog & Anthony-Twarog 1993). After these considerations, the offsets can be calculated; they are listed in Table 8, where "B94" and "G00" refer respectively to Bertelli's and Girardi's isochrones.

TABLE 7

ADOPTED SOLAR ZERO POINTS

| $M_V$ | $(B-V)_\odot$ | $(V-R)_\odot$ | $(V-I)_\odot$ |
|---|---|---|---|
| 4.84 | 0.65 | 0.37 | 0.70 |

TABLE 8

OFFSETS OF PADOVA ISOCHRONES

| | $\Delta M_V$ | $\Delta(B-V)$ | $\Delta(V-R)$ | $\Delta(V-I)$ |
|---|---|---|---|---|
| B94 | −0.056 | −0.030 | −0.010 | −0.030 |
| G00 | −0.018 | −0.023 | −0.008 | −0.026 |

### 4.2. *About the Uncertainties in the Determination of Cluster Parameters*

When adjusting an isochrone, it is possible to constrain more precisely the reddening and distance if some estimate of the metallicity is available, which is not our case. The issue of the unknown metallicity is crucial, since it is well known that, for a given age, higher metallicities mean redder colors and larger distances. For example, if we compare the isochrones of [Fe/H] = −0.38 and +0.20 dex of Girardi et al. (2000), for $\log t = 8.6$ at $M_V \sim +0.4$, we find $\Delta(B–V) \simeq 0.085$ mag. Then, in our analysis we must account for this.

According to the investigation of Twarog et al. (1997), galactic open clusters seem to have metallicities chiefly around two mean values: (i) 0.0 dex (i.e., solar) for those clusters between $R_{\rm GC} = 6.5$ and 10 kpc, and (ii) −0.3 to −0.4 dex, for clusters at $R_{\rm GC} > 10$ kpc; in both cases, the dispersions are of about 0.1 dex. We thus must cover at least this range if we do not have any hints about the metallicity. The isochrones of Girardi et al. (2000) computed for [Fe/H]= −0.38, 0.00, and +0.20, and those

TABLE 9

ADOPTED MEAN PHOTOMETRIC ERRORS

| Cluster | $V$ | $(B-V)$ |
|---|---|---|
| NGC 2658 | 0.014 | 0.042 |
| NGC 2849 | 0.020 | 0.050 |
| NGC 3247 | 0.013 | 0.071 |

of Bertelli et al. (1994) for [Fe/H]= −0.38, solar, and +0.42, satisfy this requirement.

Next, the photometric errors must be considered. They depend on the filter, detector, exposure time, and observing conditions. Their general behavior is illustrated by the mean error bars plotted in Fig. 2: at first they grow slowly with increasing $V$, until a point is reached from which they grow fast, since the errors go as the inverse of the square root of the number of object counts (Newberry 1991). If we adopted the representative photometric error of $V$ or $(B-V)$ to be equal to the maximum error, i.e., that of the faintest magnitudes, we would be largely overestimating the uncertainty in the reddening, since in general the lower sequences are not used in the fit. We then think it is safe to define the "photometric error" of $V$ and $(B-V)$ to be half the sum of the minimum and maximum error bars. Table 9 gives an account of these errors.

With these considerations, we adopt as the cluster reddening that resulting from the fitting of the intermediate set of isochrones (i.e., that corresponding to [Fe/H] = 0.0), while its uncertainty is defined by the fits of the isochrones of lower and higher metallicity, plus the mean photometric error in $(B-V)$.

The apparent distance modulus and its error can be defined analogously. However, the calculation of the *true* modulus introduces two additional factors: the reddening and the ratio of total to selective extinction $R$, through the relation $A_V = R \times E(B-V)$.

In order to obtain the uncertainty of the true modulus, the errors of these have to be combined with that of the apparent modulus by means of the method of propagation of errors. For $R$, we take the standard value for the diffuse interstellar medium, viz. $R = 3.1 \pm 0.1$.

Lastly, we define the cluster age to be that resulting from the best fit among the isochrones of solar metallicity, according to our opinion. The uncertainty of the age is in turn given by the youngest and oldest isochrones, among all those used.

### 4.3. *NGC 2658*

The main sequence of this cluster is well populated, long, and relatively well defined. In particular, we note that the upper sequence shows some dispersion, and the low part seems to be contaminated by field stars (cf. the comparison field diagram in Fig. 2).

A plot of a smaller area reveals, however, a cleaner sequence. In Figures 4 to 6 we show the $V$ versus $(B-V)$ diagram of NGC 2658 for stars observed twice (cf. § 3) and up to 2′ from the center. In each figure, several isochrones of a given metallicity are plotted; the isochrones have been chosen to try to cover the dispersion observed in the upper main sequence. The parameters that result from the fits are listed in Table 10. Our "best fit" among the solar-metallicity isochrones is that for $\log t = 8.50$, and it is plotted in solid line in Fig. 5. Following the considerations about the errors (§ 4.2), the adopted age for this cluster, corresponding to $\log t = 8.50^{+0.25}_{-0.05}$, is $3.16^{+2.46}_{-0.34} \times 10^8$ yr. Considering only the variation in metallicity, the reddening is $0.35^{+0.01}_{-0.06}$, but the introduction of the photometric errors (Table 9) brings the final adopted reddening to $E(B-V) = 0.35^{+0.05}_{-0.10}$. In the same way, the derived apparent distance modulus is $14.40^{+0.03}_{-0.41}$, the true distance modulus is $13.32^{+0.31}_{-0.52}$, and the distance is $4.6^{+0.7}_{-1.1}$ kpc. Adopting $R_\odot = 8.5$ kpc, the cluster is at $\sim 490$ pc below the galactic plane, and at $\sim 10.7$ kpc from the galactic center.

In order to derive the reddenings in $(V-R)$ and $(V-I)$, we can take advantage of the well-known results for Johnson-Cousins photometry, viz. $E(V-R)/E(B-V) \simeq 0.63$, (Alcalá & Arellano Ferro 1988), and $E(V-I)/E(B-V) \simeq 1.25$ (Dean, Warren, & Cousins 1978). In this way we obtain $E(V-R) = 0.22$ and $E(V-I) = 0.44$, with errors in each case that amount at least to those of $E(B-V)$. The $V$ versus $(V-R)$ and $(V-I)$ diagrams of NGC 2658 are plotted in Figure 7, showing the corresponding isochrones that have been shifted by the reddenings just estimated. It can be seen that the isochrones follow closely the shape of the sequences, though they are not located exactly on them; however, the uncertainty in the reddenings sufficiently account for this difference. Finally, the total extinction $A_V = 3.1 \times E(B-V)$ turns out to be $1.09^{+0.16}_{-0.31}$ mag.

To estimate the apparent size of the cluster, we can compare the profiles of distribution of stars for both the cluster and comparison fields. By means of a well-known procedure that uses the IRAF task named ADDSTAR, it is found that $\sim 100\%$ of stars

TABLE 10

PARAMETERS OF NGC 2658

| [Fe/H] | $\log t$ | $E(B-V)$ | $(m-M)$ |
|---|---|---|---|
| −0.38 | 8.55–8.75 | 0.36 | 14.00 |
| solar | 8.45–8.65 | 0.35 | 14.40 |
| +0.20 | 8.55–8.65 | 0.29 | 14.42 |

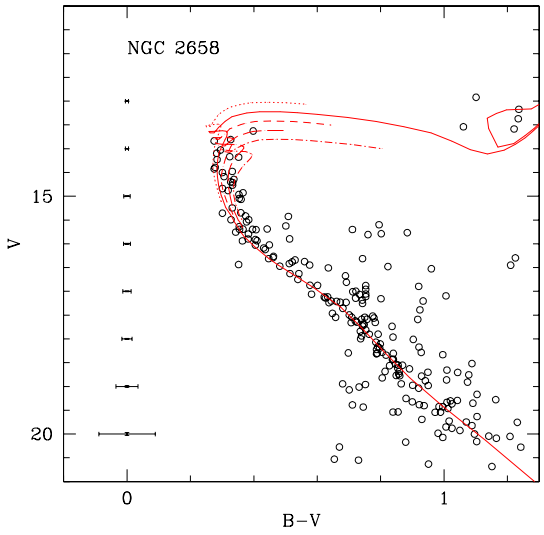


Fig. 4. Color-magnitude diagram of NGC 2658 for stars inside a radius of 2′ from the cluster center, and observed twice. The isochrones by Girardi et al. (2000) are of composition ($Y = 0.25$, $Z = 0.008$). From left to right, the isochrones correspond to $\log t = 8.55$, 8.60 (solid line), 8.65, 8.70, and 8.75. In this and the two following figures, the isochrones are shifted as indicated in Table 10.

down to $V \sim 17.5$ are detected by DAOPHOT in typical ($\sim$ 60 sec) CASLEO $V$ frames. Down to that limit, the number of stars per $V$ interval, in concentric zones centered on the cluster, is compared with the average number of stars in the same interval of $V$ in the comparison field. This comparison is shown in Figure 8, where it can be seen that an excess of cluster stars can be observed even for the last zone (3′ < radius < 4′), so the cluster must extend beyond that limit.

### 4.4. *NGC 2849*

This cluster has a small apparent size, and its diagrams show, as expected, strong field star contamination (cf. Fig. 2). A plot of the central stars does not, however, reveal a definite sequence. In Figure 9 we show the color-magnitude diagrams for stars

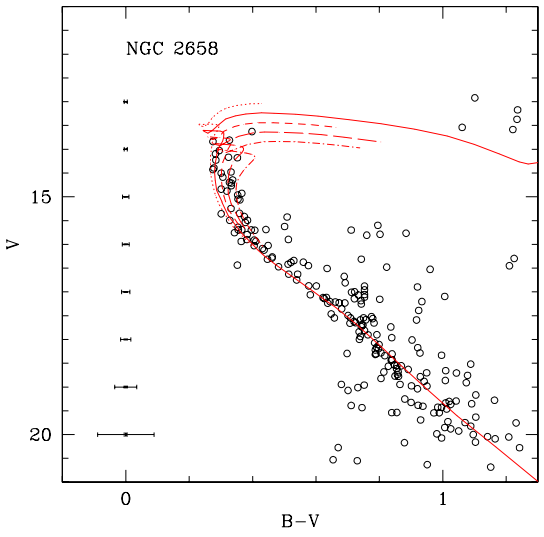


Fig. 5. Same stars as in Fig. 4, but now the isochrones are of solar ($Y = 0.273$, $Z = 0.019$) metallicity. From left to right, they correspond to $\log t = 8.45$, 8.50 (solid line), 8.55, 8.60, and 8.65.

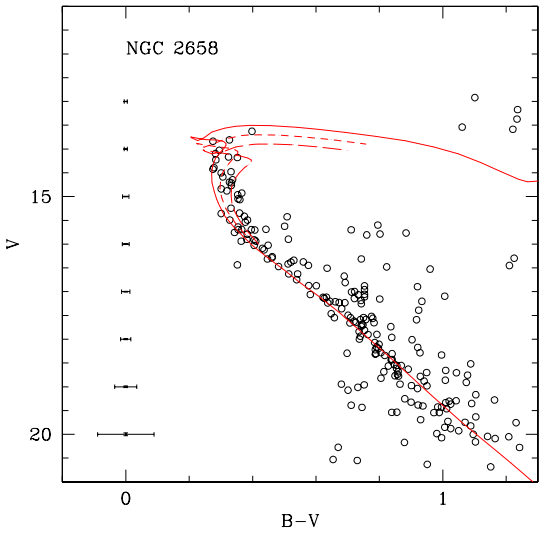


Fig. 6. Same stars as in Fig. 4, but the isochrones are of composition ($Y = 0.30$, $Z = 0.03$). From left to right, the isochrones correspond to $\log t = 8.55$ (solid line), 8.60, and 8.65.

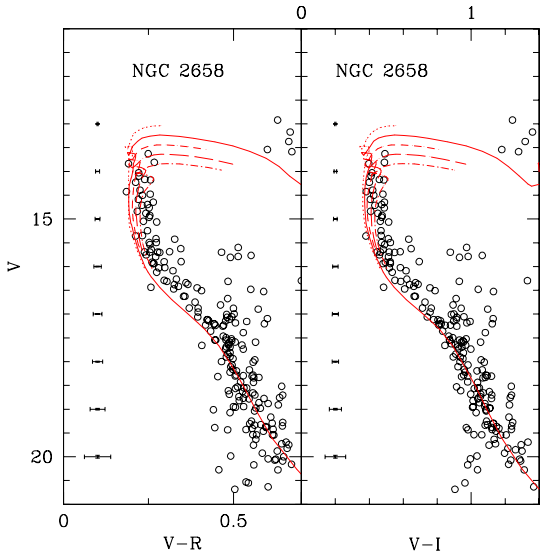


Fig. 7. $V$ versus ($V$–$R$) and ($V$–$I$) diagrams of NGC 2658. The stars and isochrones plotted are the same as in Fig. 5.

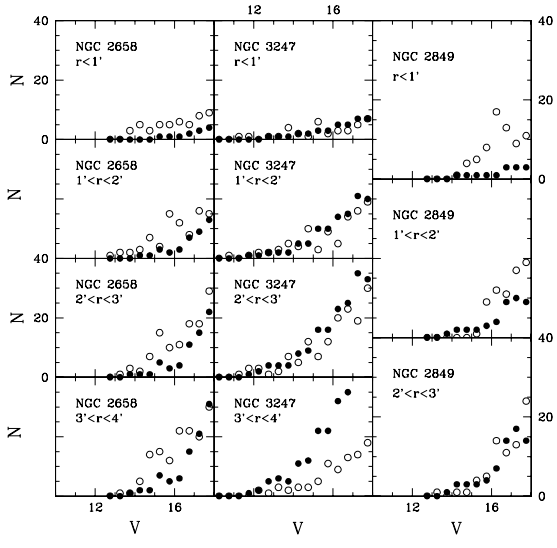


Fig. 8. Number of stars, per magnitude interval, of cluster and comparison fields, in circular, concentric areas, starting from the center (upper panels) and proceeding outwards; each column corresponds to a cluster. Open circles: cluster stars; solid circles: comparison-field stars.

around 1′ of the center, and for stars between 1′ and 1.5′. It can be seen that the last stars more clearly define the cluster sequence, while the others appear mainly as a redder, dispersed sequence. We interpret this effect as caused by differential reddening, with somewhat higher values at the center. We use therefore, the stars in 1–1.5′ in our analysis (Figures 10 to 12), with the caveat that the derived reddening has to allow for the observed range, which we estimate to be about 0.11 mag (cf. Fig. 11).

The resultant parameters from the fits are listed in Table 11; the tabulated reddenings are lower limits. Our best fit is that for $\log t = 8.8^{+0.1}_{-0.05}$, or $6.31^{+1.6}_{-0.7} \times 10^8$ yr. As discussed above, the reddening may be variable and cover a wide range. Considering only the analysis performed with solar isochrones, $E(B-V)$ can vary from 0.46 to at least 0.57. Moreover, the sum of the uncertainties in metallicity and photometry is 0.12 mag. In order to derive the true modulus, however, we have only to consider the minimum reddening (i.e., 0.46). In this way, and assuming 0.12 mag as the error of $E(B-V)$, we calculate an apparent modulus of $15.45^{+0.02}_{-0.15}$, and a true modulus of $14.02^{+0.38}_{-0.40}$ or, equivalently, a distance of $6.4^{+1.1}_{-1.2}$ kpc. The cluster thus appears to be at $\sim$ 11 kpc from the galactic center and at $\sim$ 700 pc above the plane.

The extinction $A_V$ is in the range 1.4–1.8 $\pm$ 0.3 mag, the reddening in $(V-R)$ goes from 0.29 to 0.36, and the reddening in $(V-I)$ is between 0.58 and 0.71, with errors at least of 0.12 mag. Figure 13 shows the $V$ versus $(V-R)$ and $(V-I)$ diagrams of NGC 2849, shifted 0.29 and 0.58 mag, respectively. As in the case of NGC 2658, the isochrones are not located exactly on the observed sequences, but again, the uncertainty in the reddenings can explain that, assuming that the relations between the reddenings are standard.

Given the small size of NGC 2849, and since we did not observe a comparison field, we adopt as such the cluster field beyond 3′ of the center (cf. Fig. 2). Through an analysis similar to that performed for NGC 2658, it is found that at 2′–3′ from the center the distribution of stars relative to that of the comparison field are similar (cf. Fig. 8), so the cluster has a radius of at most 2′, as defined by the stars down to $V \sim 17.5$ mag.

### 4.5. *NGC 3247*

The lower main sequence is not very well defined, but the upper part is long, bright, and well defined, albeit sparsely populated.

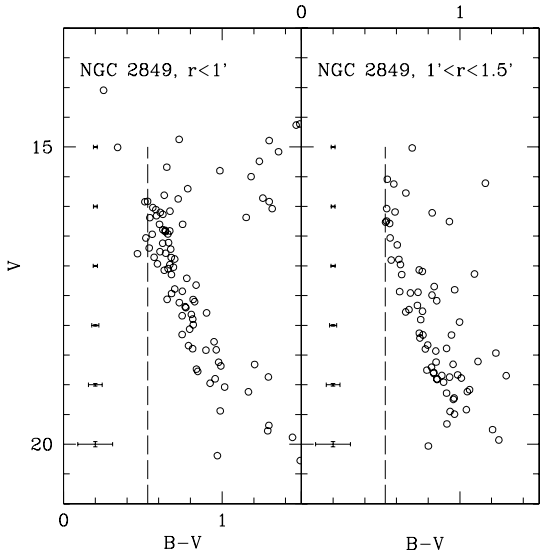


Fig. 9. Color-magnitude diagrams of NGC 2849, for central stars (left), and between $1'$ and $1.5'$ (right). The dashed, vertical line is drawn for reference.

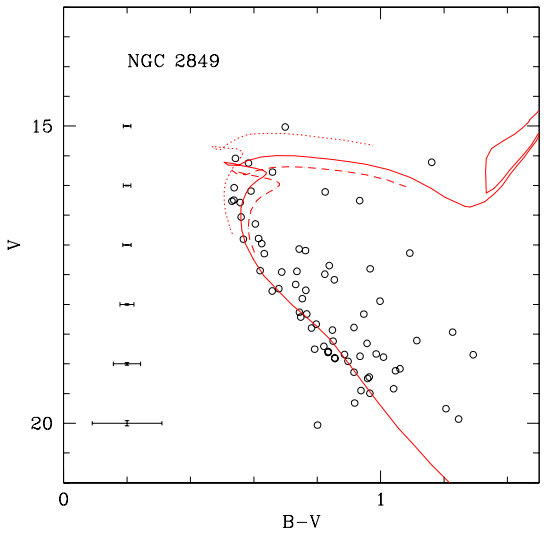


Fig. 10. Color-magnitude diagram of NGC 2849 for stars between $1'$ and $1.5'$ from the center. The composition of the isochrones is ($Y = 0.25$, $Z = 0.008$); from left to right, they correspond to $\log t = 8.75$, 8.85 (solid line), and 8.90. In Figs. 10-12 the isochrones are shifted as indicated in Table 11.

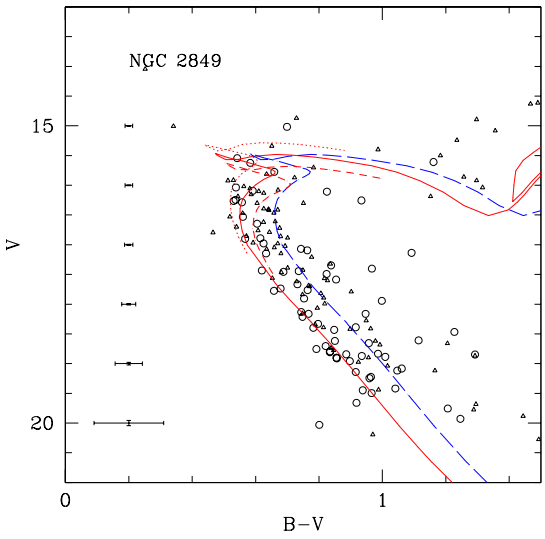


Fig. 11. Diagram of NGC 2849 for all stars inside $1'$ (small triangles), and between $1'$ and $1.5'$ (circles). The isochrones are of solar metallicity ($Y = 0.273$, $Z = 0.019$), and from left to right, they correspond to $\log t = 8.75$, 8.80 (solid line), and 8.85. The isochrone of $\log t = 8.80$ is again plotted with an extra shift of 0.11 mag to the red.

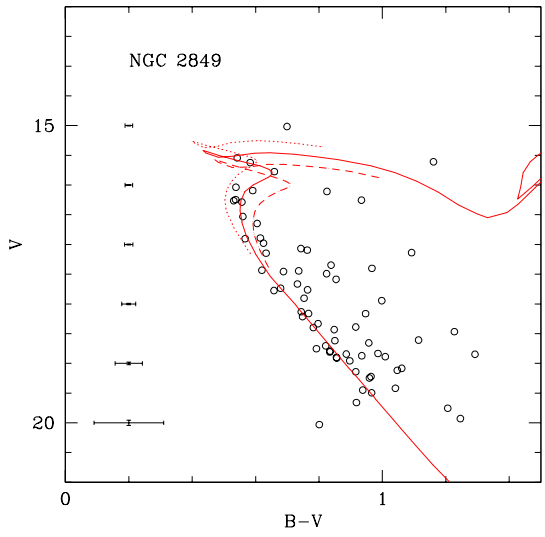


Fig. 12. Diagram of the same stars as in Fig. 10, but now the isochrones are of composition ($Y = 0.30$, $Z = 0.03$), and correspond, from left to right, to $\log t = 8.75, 8.80$ (solid line), and 8.85.

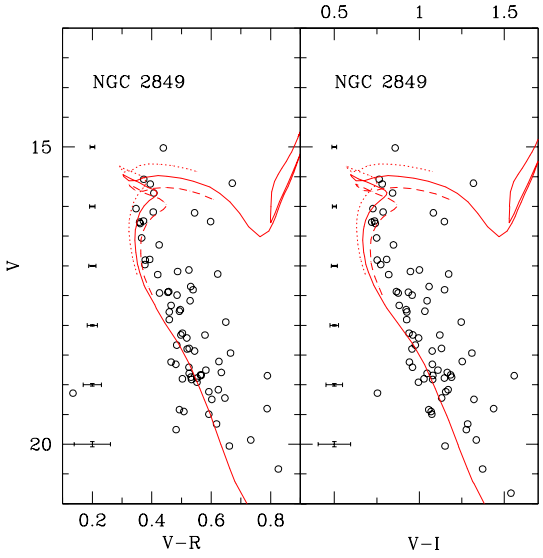


Fig. 13. Diagrams of NGC 2849 plotting $V$ versus ($V$–$R$) and ($V-I$). Stars are those between 1′ and 1.5′ from the center; the isochrones are of solar composition and $\log t = 8.75$, 8.80 (solid line), and 8.85. See the text for the reddenings in these colors.

TABLE 11

PARAMETERS OF NGC 2849

| [Fe/H] | $\log t$ | $E(B-V)$ | $(m-M)$ |
|---|---|---|---|
| −0.38 | 8.75–8.90 | 0.53 | 15.32 |
| solar | 8.75–8.85 | 0.46 | 15.45 |
| +0.20 | 8.75–8.85 | 0.39 | 15.38 |

As the cluster seems rather young, we use the isochrones by Bertelli et al. (1994) (cf. § 4.1) in our analysis. The fits of isochrones of different metallicities in the $V$ versus ($B-V$) diagrams of NGC 3247 are shown in Figures 14 to 16. Our best fit among the solar isochrones corresponds to $\log t = 7.60$, plotted as a solid line in Figure 15. Considering the whole range of ages (cf. Table 12), we adopt for NGC 3247 the age given by $\log t = 7.6^{+0.4}_{-0.3}$, or $4^{+6}_{-2} \times 10^7$ yr. Apparently, different reddenings are not required when changing the metallicity, but the assigned error in the photometry is considerable ($\sim$ 0.07 mag), and is thus the principal source of error in the reddening, which then amounts to $0.39 \pm 0.07$. The apparent distance modulus is $13.10^{+0.46}_{-0.39}$; the true modulus is $11.89^{+0.51}_{-0.45}$, and the distance is $2.4^{+0.6}_{-0.5}$ kpc. NGC 3247 is located at $\sim$ 8.2 kpc from the galactic center, and at $\sim$ 14 pc below the plane.

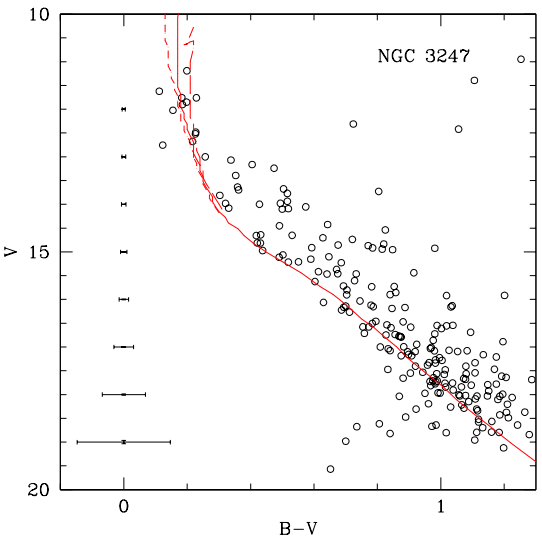


Fig. 14. Color-magnitude diagram of NGC 3247 for stars up to 2.5′ from the center. The isochrones by Bertelli et al. (1994) are of composition ($Z$ = 0.008, $Y$ = 0.25). From left to right, the isochrones correspond to $\log t = 7.5$, 7.70 (solid line), and 8.1. In Figs. 14-16 the isochrones are shifted as indicated in Table 12.

TABLE 12

PARAMETERS OF NGC 3247

| [Fe/H] | $\log t$ | $E(B-V)$ | $(m-M)$ |
|---|---|---|---|
| −0.38 | 7.5–8.0 | 0.39 | 12.70 |
| solar | 7.3–7.9 | 0.39 | 13.10 |
| +0.42 | 7.5–7.9 | 0.39 | 13.55 |

The total extinction $A_V$ is $1.21 \pm 0.22$ mag. The reddening in ($V-I$) is $0.49 \pm 0.07$ [again, this error is a lower limit, given by that of $E(B-V)$]. Figure 17 shows the $V$ versus ($V-I$) diagram of NGC 3247, with the same isochrones as in Fig. 15. Unlike the preceding clusters, the isochrone follows the observed sequence fairly well in shape and position.

The comparison of the distribution of stars of the cluster frames with that of the comparison field shows little excess of cluster stars above the comparison field stars, since the cluster is not very rich (Fig. 8). However, the clear excess of field stars in the area 3′–4′ suggests a limit of $\sim$ 3′ for NGC 3247, as defined by stars down to $V \sim 17.5$.

## 5. CONCLUSIONS

We have presented new CCD photometry of the relatively poorly studied galactic open clusters

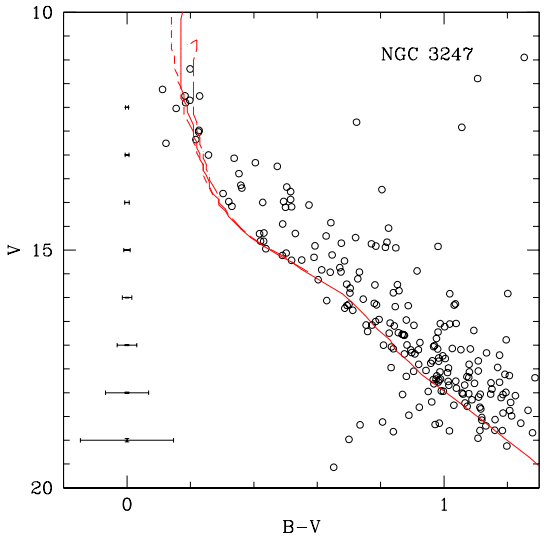


Fig. 15. Same stars as in Fig. 14, but here the isochrones are of solar composition ($Z = 0.02$, $Y = 0.28$). From left to right, the isochrones correspond to $\log t = 7.3$, 7.6 (solid line), and 7.9.

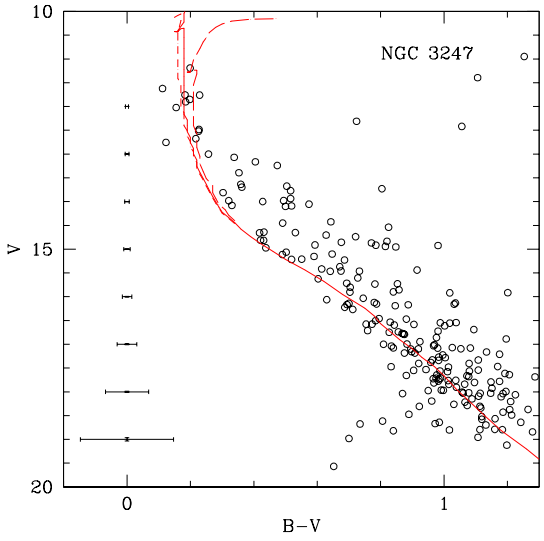


Fig. 16. Same stars as in Fig. 14, but now the isochrones are of composition ($Z = 0.05$, $Y = 0.352$). From left to right, the isochrones correspond to $\log t = 7.5, 7.6$ (solid line), and 7.9.

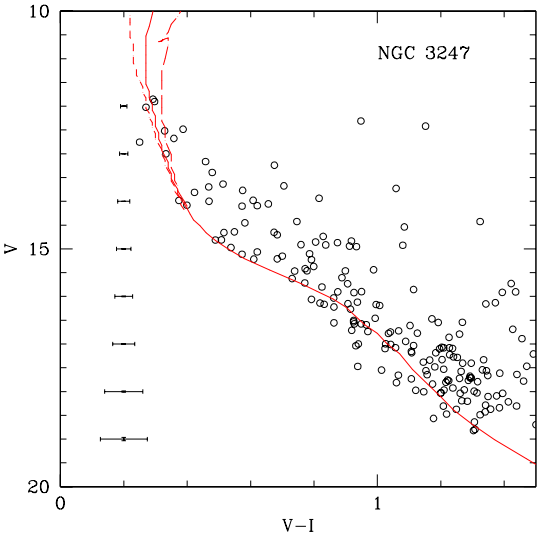


Fig. 17. $V$ versus $(V-I)$ diagram for NGC 3247, with the same stars and isochrones plotted in Fig. 15. The isochrones are shifted 0.49 mag in color.

NGC 2658, NGC 2849, and NGC 3247. We have used the Padova isochrones of three different metallicities to constrain the cluster parameters.

In order to tie our results to those of, and in the manner suggested by, for instance, Twarog et al. (1997), we have renormalized the Padova isochrones to the solar values $(B-V)_\odot = 0.65$ and $M_V = 4.84$; by means of the calibrations of Alonso et al. (1996) we have also derived the appropriate solar colors in the indexes $(V-R)$ and $(V-I)$. The colors, that we propose as zero points for renormalizing the isochrones are $(V-R)_\odot = 0.37$ and $(V-I)_\odot = 0.70$. Once this is established, the offsets for the Padova isochrones turn out to be: (i) for Bertelli et al. (1994), −0.056 mag in $M_V$, −0.030 in $(B–V)$, −0.010 in $(V–R)$, and −0.030 in $(V–I)$; (ii) for Girardi et al. (2000), −0.018 mag in $M_V$, −0.023 in $(B–V)$, −0.008 in $(V–R)$, and −0.026 in $(V–I)$.

By means of our analysis, we have derived the following cluster parameters. For NGC 2658, a reddening of $E(B-V) = 0.35^{+0.05}_{-0.10}$, $\log(\text{age}) = 8.50^{+0.25}_{-0.05}$, a true distance modulus $(m-M)_0 = 13.32^{+0.36}_{-0.52}$, and a distance of $= 4.6^{+0.7}_{-1.1}$ kpc. For NGC 2849, the reddening is in the range (0.46–0.57)±0.12, $(m-M)_0 = 14.02^{+0.38}_{-0.40}$, the distance is $6.4^{+1.1}_{-1.2}$ kpc, while $\log(\text{age}) = 8.8^{+0.1}_{-0.05}$. Finally, for NGC 3247 we have obtained $E(B-V) = 0.39 \pm 0.07$, $\log(\text{age}) = 7.6^{+0.4}_{-0.3}$, $(m-M)_0 = 11.89^{+0.51}_{-0.45}$, and a distance of $= 2.4^{+0.6}_{-0.5}$ kpc.

The author acknowledges use of the CASLEO CCD and data acquisition system supported under US National Science Foundation grant AST-90-15827 to R. M. Rich. It is a pleasure to thank Dr. B. Twarog for his useful comments, Dr. H. Levato (CASLEO), Dr. R. Garrison (UTSO), and their staffs for allowing the use of the facilities, and Messrs A. de Franceschi, B. Duffee, R. Jakowczyk, and V. Mulet, for their assistance at the telescopes. Finally, it is only too fair to thank the anonymous referee for the many improvements suggested.

## REFERENCES

Alcalá, J. M., & Arellano Ferro, A. 1988, Rev. Mex. Astron. Astrof., 16, 81
Alonso, A., Arribas, S., & Martínez-Roger, C. 1996, A&A, 313, 873
Bertelli, G., Bressan, A., Chiosi, C., Fagotto, F., & Nasi, E. 1994, A&AS, 106, 275
Bessell, M. S. 1983, PASP, 95, 480
Dean, J. F., Warren P. R., & Cousins, A. W. J. 1978, MNRAS, 183, 569
Girardi, L., Bressan, A., Bertelli, G., & Chiosi, C. 2000, A&AS, 141, 371
Golay, M. 1974, Introduction to Astronomical Photometry (Dordrecht: D. Reidel Publishing Company), 110
Graham, J. A. 1982, PASP, 94, 244
Grubissich C. 1977, A&AS, 29, 379
Lyngå, G. 1987, Lund Catalogue of Open Cluster Data, Fifth Edition (Strasbourg: Centre de Données Stellaires)
Mermilliod, J.-C. 1995, in Information and On-Line Data in Astronomy, eds. D. Egret & M. A. Albrecht (Dordrecht: Kluwer Academic Press), 127
Newberry, M. V. 1991, PASP, 103, 122
Ramsay G., & Pollaco D. L. 1992, A&AS, 94, 73
Stetson, P. B. 1987, PASP, 99, 191
Stetson, P. B. 1990, PASP, 102, 932
Twarog B. A., & Anthony-Twarog B. J. 1989, AJ, 97, 759
Twarog B. A., & Anthony-Twarog B. J. 1993, PASP, 105, 78
Twarog B. A., Ashman K. M., & Anthony-Twarog B. J. 1997, AJ, 114, 2556
VandenBerg, D. A., & Poll H. F. 1987, AJ, 98, 1451



Javier A. Ahumada: Observatorio Astronómico, Universidad Nacional de Córdoba, Laprida 854, 5000 Córdoba, Argentina (javier@oac.uncor.edu).